Int J Adv Manuf Technol (2016) 85:869–879
DOI 10.1007/s00170-015-7977-2

ORIGINAL ARTICLE

Effects of flow stress behaviour, pressure loading path and temperature variation on high-pressure pneumatic forming of Ti-3Al-2.5V tubes

Gang Liu [1,2] · **Jianlong Wang** [1] · **Kexin Dang** [1] · **Shijian Yuan** [1,2]

Received: 1 May 2015 / Accepted: 12 October 2015 / Published online: 27 October 2015

Abstract High-pressure pneumatic forming (HPPF) is an internal high-pressure forming process at elevated temperatures, which is based on quick plastic forming (QPF), hot metal gas forming (HMGF) and hydroforming. In this study, the HPPF experiments were performed on Ti-3Al-2.5V tubes using a square cross-sectional die at higher pressure levels and lower temperatures. The uniaxial tensile tests were carried out at various temperatures and strain rates before the HPPF experiments. The flow stress of Ti-3Al-2.5V tubes is evidently affected by both temperature and strain rate. Because of this, the corner radii all change linearly over time at the pressurization stage but exponentially over time at the constant pressure stage. The cooling effect of the inflow process on the tubes results in temperature differences between the centre of the straight wall areas and the corner areas of the tubes during the inflow process. Adopting the lower pressurization rate and filling regenerative materials into the tube are effective methods for decreasing or eliminating the temperature difference.

Keywords High-pressure pneumatic forming · Strain rate · Corner filling · Temperature difference

✉ Gang Liu
gliu@hit.edu.cn

[1] College of Materials Science and Engineering, Harbin Institute of Technology, Harbin 150001, China

[2] National Key Laboratory for Precision Hot Processing of Metals, Harbin Institute of Technology, Harbin 150001, China

1 Introduction

Titanium and its alloys have become very important commercially over the past 50 years due to their low density, good strength-to-weight ratio, excellent corrosion resistance and good mechanical properties [1]. They have been widely used in the fields of aerospace, chemical processing, marine and offshore, transportation, medicine, etc. Plastic forming has been the most applicable forming route for titanium components, which cannot only reduce the cost due to machining but also enhance the performance of the products [2]. However, titanium alloys are often considered more difficult to form than other metallic alloys, such as steel and aluminium, because of their high yield stress and low elastic modulus. As a potential solution to counter the disadvantages mentioned above, the use of elevated temperatures as a process parameter in forming operations is suggested [3].

Huang et al. experimentally studied the quasi-static (10^{-3} s^{-1}, 10^{-2} s^{-1}) tensile behaviour of a CP-Ti plate at elevated temperatures (25–700 °C) and found that the total elongation presented a complex changing trend with the increase of temperature [4]. Tsao et al. studied the flow stress behaviour of CP-Ti sheets by uniaxial warm tensile testing at temperatures ranging from 350 to 500 °C and strain rates from 8.3×10^{-3} to 5.0×10^{-2} s^{-1}. They established a constitutive model using the Fields-Backofen (FB) equation to describe the flow stress behaviour [5]. Zhang et al. also established the constitutive equations and revised the expression of strain hardening exponent n, strain rate sensitivity parameter m and strength coefficient K by studying the quasi-static tensile behaviour of bent large diameter, thin-walled (LDTW) CP-Ti tubes [6]. Based on the research above, it can be concluded that sheet metal forming of titanium at elevated temperatures is affected by temperature and strain rate at the same time. In the high-pressure pneumatic forming (HPPF) process of Ti-3Al-2.5V

alloy, uniaxial tensile testing at elevated temperatures should be done first to gain a fundamental understanding of formability with respect to temperature and strain rate.

Hot forming processes are useful for improving the formability of work pieces having low ductility at room temperature. As a hot forming process with huge potential, pneumatic forming processes have been widely studied in the past 10 years. Luo et al. presented a novel SPF process utilizing a mechanical preforming operation of SPF5083 alloy and verified that this process could deliver a superior thickness profile as compared to conventional SPF [7]. Based on the two-stage SPF process, Luckey Jr. et al. designed a preform die to improve the thickness profile of SPF5083 alloy parts [8]. Luo et al. also compared two-stage gas forming (TSGF) and hot draw mechanical preforming (HDMP) to conventional SPF when forming a SPF5083 alloy part and found that HDMP could provide a superior thickness profile and faster forming cycle than the other two processes [9]. Liu et al. combined deep drawing and blow forming into one operation. Together with a non-isothermal heating system, they successfully formed Ti-6Al-4V alloy sheets at 800 °C in 16 min [10]. Tang used hot-bend assisted gas forming (HBAGF) to fabricate aluminium airplane strakelets with improved thickness profiles [11]. Based on the research above, it can be seen that blow preforming and mechanical preforming are effective ways to improve thickness profiles in the pneumatic forming process. Based on hot stamping and hydroforming processes, a pneumatic forming process with higher pressure (usually above 15 MPa) was developed for high-strength materials. Neugebauer et al. used a pneumatic forming device with the maximum pressure of 80 MPa to form 22MnB5 high-strength steel tubes with integrated heat treatment [12]. Elsenheimer et al. set up hot tube bulge test equipment with the maximum pressure of 35 MPa to obtain stress-strain curves at elevated temperatures [13]. Drossel developed a measuring instrument to determine the gas temperature curve during pneumatic forming processes and to analyse the influence of gaseous medium with high pressure on the cooling process of work pieces [14]. Liu et al. presented a HPPF process based on QPF, HMGF and hydroforming [15]. With the maximum pressure of 30 MPa, they also successfully formed Ti-alloy components with irregular cross-sections and square cross-sections at 850 °C [15, 16].

In the present study, the HPPF process of Ti-alloy hollow parts with square cross-sections was developed further at higher pressure levels and temperatures ranging from 650 to 800 °C. The circumferential expansion ratio of the die cavity was increased to 20 % to avoid the preforming process during closing the die and the corner-filling behaviour could be studied better. The flow stress behaviour of Ti-3Al-2.5V tubes were also studied using uniaxial tension tests at temperatures ranging from 650 to 800 °C and strain rates ranging from 0.001 s^{-1} to 0.1 s^{-1}. The effects of pressure loading path and temperature on corner-filling behaviour were investigated further, and the corner-filling curves were fitted more accurately. The influence of the inflow process of gaseous media with high pressure on tube temperature was studied, which was inspired by the work of Drossel et al. [14]. The corner-filling time and thickness profiles of the fully formed tubular components under different forming conditions were also discussed.

2 Experimental details

2.1 High-pressure pneumatic forming system and components

Based on the previous work of Liu et al. [15], the HPPF system was further developed in this study. The system is composed of a gas pressure generator unit, a gas pressure management unit and an induction heating unit. The gas pressure generator unit is able to apply a theoretical gas volume of 1×9 L with the maximum pressure of 70 MPa. The gas pressure management unit applies a user-defined pressure versus time relationship to form the tube and provides accurate pressure control within ±3 % of the target pressure. Laser displacement sensors, thermocouples and a data acquisition module for temperature are also embedded in the gas pressure management unit. Laser displacement sensors are used to monitor and record the bulge height of the tube during the forming process. Thermocouples and the data acquisition module for temperature are used to monitor and record the die and tube temperatures during the heating and forming processes. The induction heating unit is able to heat the die to the forming temperature rapidly and the induction coils were designed according to the shape of the die.

The round-to-square die set was designed and manufactured for the HPPF experiments. The pneumatic forming process in the die cavity with circumferential expansion ratio of 20 % was analysed in this study. The cross-section of the die cavity is shown in Fig. 1, which is almost the same size as the initial outside diameter of the tube. There is no preforming process while closing the die, and this is a typical cross-section for a corner-fill test in the internal high-pressure forming process.

2.2 Uniaxial tensile tests at elevated temperatures

Ti-3Al-2.5V (ASTM Gr. 9) titanium alloy seamless tubes that were 40 mm in outer diameter, 200 mm in length and 2 mm in thickness were used in this study. The curved Ti-3Al-2.5V tube specimens were designed and wire cut directly along the longitudinal direction of the tube, as shown in Fig. 2. The tensile tests were carried out on an Instron 1361 testing machine at temperatures ranging from 650 to 800 °C. Three

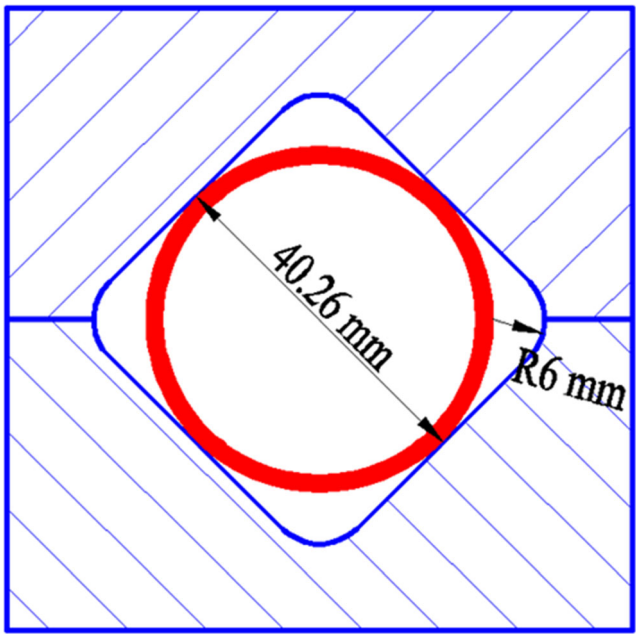

Fig. 1 The cross-section of the die cavity with circumferential expansion ratio of 20 %

nominal strain rates of 0.001, 0.01 and 0.1 s^{-1} were applied between 650 and 800 °C at intervals of 50 °C. For accuracy and repeatability, the tensile tests were repeated at least twice at each condition. To get a homogenous temperature distribution, three thermocouples were used and attached to the top side, central part and bottom side of the gauge. Prior to testing, all specimens were polished to remove any major scratches in order to prevent fractures at undesired locations, and oxidation was prevented by painting water glass (sodium silicate) on the specimens. Under constant temperatures, the specimens were stretched to failure, and then the engineering stress-strain relations were obtained.

2.3 High-pressure pneumatic forming

HPPF experiments were carried out at various temperatures and pressure loading paths. Boron nitride was chosen as the lubricant during the HPPF experiments. It was also sprayed on the inner surface of the tube to prevent oxidation. In order to investigate the effects of forming pressure on the corner-filling behaviour at relatively lower temperatures, four different pressure loading paths were used in HPPF experiments at 700 °C, which were programmed into the gas pressure management unit. The gas pressure would hold constant as soon as it reached the designated value, and the total forming time was within 300 s. HPPF experiments were also carried out at various temperatures to further explore corner-filling behaviour. Using the same defined pressurization profiles, the corner was formed, respectively, at temperatures of 650, 700, 750 and 800 °C. The forming times were within 300 s. During the HPPF experiments, A KEYENCE laser displacement sensor was used to measure the displacement of the horizontal corner of the square zone in real time, as shown in Fig. 3. The data recorded was used to calculate the horizontal corner radius in real time. During the corner-filling process, the instantaneous radius and displacement of the corner can be expressed as Eq. 1.

$$r = R + 0.414\Delta L \tag{1}$$

where r is the instantaneous radius of the corner, R is the radius of the die and ΔL is the instantaneous displacement of the corner.

In order to investigate the effect of the inflowing gas on the tube temperature, the temperature at the centre of the horizontal corner was measured and recorded during the pneumatic forming process. This is because corner area came into contact with die cavity finally and it was convenient to insert the thermocouple in the horizontal direction. At the same time, the temperature at the straight wall area of the die cavity was measured and recorded because the tube would come into contact with the straight wall area first and the temperature would be in accordance with the die's temperature immediately. The temperature-measuring method is also shown in Fig. 3. In this case, two calibrated, type K thermocouples from Omega Engineering Inc. with diameters of 0.5 mm were used. It was very hard to spot-weld the thermocouple onto the titanium tube tightly, and the thermocouple failed away from the tube easily during the HPPF process, so a compressed spring force (F_s) was applied to the thermocouple for measuring the tube temperature to keep it in contact with the tube during the pneumatic forming process. The other thermocouple was placed within the die 2 mm from the middle area of the straight

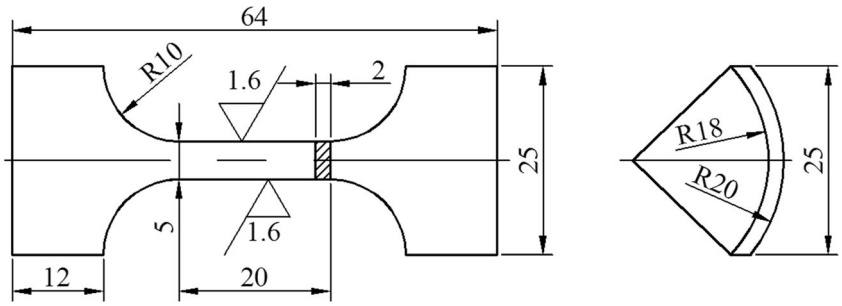

Fig. 2 Designed tensile specimen for Ti-3Al-2.5V seamless tube (units mm^{-1})

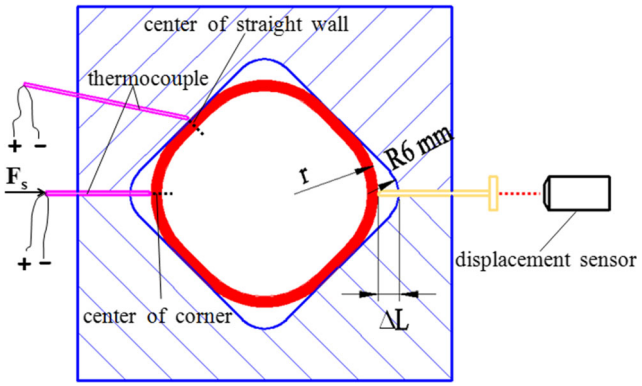

Fig. 3 Illustration of the measuring method for displacement and temperature

wall. A data acquisition module with eight differential channels from Omega Engineering Inc. was used to record the temperature data. The acquisition frequency was 10 Hz. Based on the preparation above, two pressure loading paths with different pressurization rates were used in the HPPF experiments at 700 °C. The gas pressure would hold constant as soon as it reached the designated value, and it would not be released until the tube came into total contact with the die cavity. Tubes filled with ceramic balls of Φ 8 mm were also bulged with the same pressure loading paths as comparisons.

3 Results and discussion

3.1 Tensile behaviour of Ti-3Al-2.5V alloy tube

Figure 4 shows the true stress-strain curves of Ti-3Al-2.5V alloy tubes from the tensile tests at temperatures ranging from 650 to 800 °C and strain rates of 10^{-3}, 10^{-2} and 10^{-1} s^{-1}. It can be seen that both temperature and strain rate have pronounced effects on the flow stress of Ti-3Al-2.5V alloy tubes. As expected, the flow stress decreases with increasing temperatures and decreasing strain rates. At 650 °C and under a strain rate of 10^{-1} s^{-1}, the flow curve exhibits the power-law constitutive relation obviously until peak stress is reached, at which level a softening region leading to fracture is observed [17]. At 800 °C and under a strain rate of 10^{-3} s^{-1}, the flow curve has a slight drop when the strain is increased through thermal softening [6]. A lower hardening effect and a longer softening region leading to fracture were noted when testing at a higher temperature and a lower strain rate. The results indicate that dynamic recovery and dynamic recrystallization occurred during testing. The flow behaviour variations at different deformation conditions are most likely related to the hardening and softening mechanisms. An increase in the strain rate will increase the dislocation generation rate and the accumulation rate. However, an increase in temperature will increase the dislocation annihilation rate [5, 17].

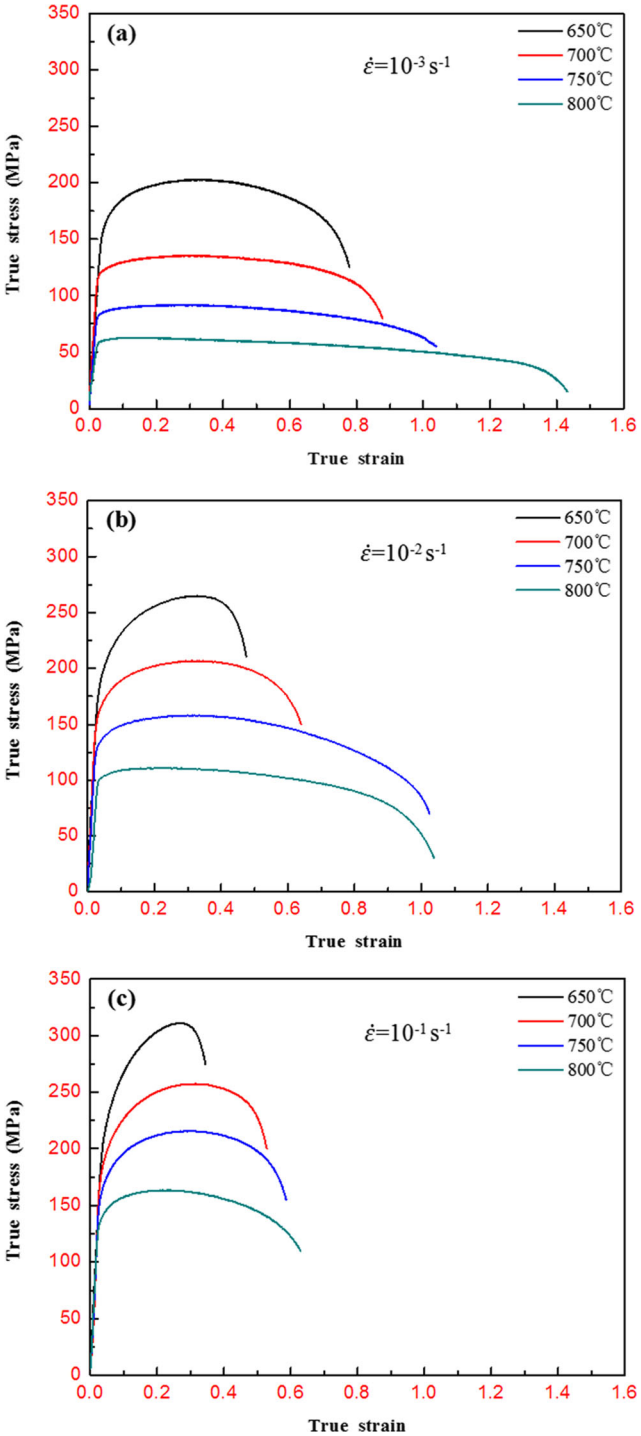

Fig. 4 True stress-strain curves of Ti-3Al-2.5V alloy tubes at various temperatures and strain rates **a** $\dot{\varepsilon}$ =10^{-3} s^{-1}, **b** $\dot{\varepsilon}$ =10^{-2} s^{-1} and **c** $\dot{\varepsilon}$ =10^{-1} s^{-1}

The effects of temperature and strain rate on fracture elongation are shown in Fig. 5. The results indicate that the fracture elongations of Ti-3Al-2.5V alloy tubes show increasing tendencies with increasing temperatures and decreasing strain rates. The minimum facture elongation is 43.6 % at the

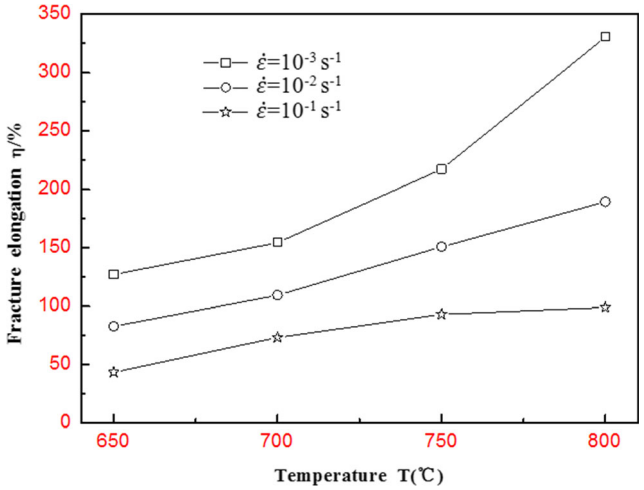

Fig. 5 Effects of temperature and strain rate on fracture elongation

temperature of 650 °C and strain rate of 10^{-1} s^{-1}. The maximum fracture elongation can reach 330.4 % at the temperature of 800 °C and strain rate of 10^{-3} s^{-1}, which is most likely the result of dynamic recrystallization. In addition, at the temperature range of 700 to 800 °C, fracture elongation is still above 70 %, even at strain rates of up to 10^{-1} s^{-1}. This indicates that this strain rate is suitable for the HPPF process of Ti-3Al-2.5V alloy tubes at temperatures below 800 °C.

The work-hardening exponent (*n* value) and the strain rate sensitivity exponent (*m* value) are not constant, varying mainly with temperature and strain rate, which are very important parameters influencing the formability of metal tubes. Based on the experimental true stress-strain data, the values of *m* and *n* were calculated according to the method Tsao et al. adopted [5]. As shown in Fig. 6, the work-hardening coefficient (*n* value) increases as the strain rate increases due to an increase of dislocation density and dislocation multiplication rate. In comparison, it decreases as the temperature increases due to an increase of shifts at boundaries for the nucleation, dislocation disappearance and the growth of DRX grains [5]. For the

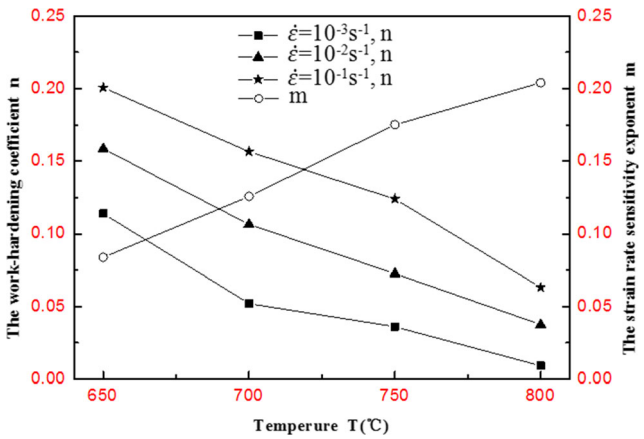

Fig. 6 Variations of *n* value with temperature at various strain rates and *m* value with temperatures

strain rate sensitivity exponent (*m* value), it generally increases as the temperature increases due to higher flowability and lower dynamic yield stress resulting from more DRX.

3.2 Corner-filling behaviour under various pressure loading paths and temperatures

Based on the further developed HPPF system, the pressure loading path can be controlled more precisely and recorded at the same time during the pneumatic forming process. As shown in Fig. 7a, the pressure loading paths with four different pressurization rates were recorded during the HPPF process at 700 °C. The pressurization rates were 1.5, 2.5, 3.5 and 4.5 MPa s^{-1}, respectively. The forming time of 300 s was divided into a pressurization time of 10 s and a constant pressure holding time of 290 s. From the recorded results, it can be concluded that the pressure can be controlled within ±3 % of the target pressure.

Table 1 shows the corner radii of the tubular components formed under various pressure loading paths at 700 °C. It can be seen that the corner radius is smaller at higher pressure

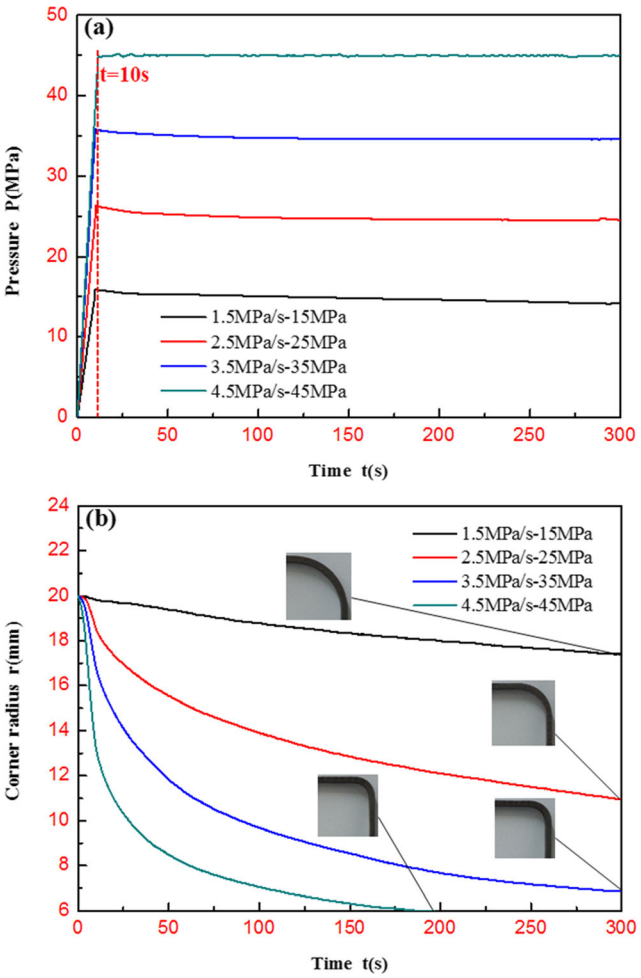

Fig. 7 **a** Pressure loading paths with four pressurization rates and **b** corner-filling curves under various pressure loading paths at 700 °C

Table 1 Corner radii under various pressure loading paths at 700 °C

Temperature (°C)	Time (s)	Pressurization rate (MPa s^{-1})	Corner radius (mm)
700	300	1.5	17.5
700	300	2.5	11
700	300	3.5	7
700	300	4.5	6

levels. The corner-filling process is shown in Fig. 7b. It indicates that the corner radius changes faster at higher pressure levels, and this result is similar to our previous work at 850 °C [15]. As is generally known, forming smaller corners requires higher pressures in conventional hydroforming processes at room temperature. When the pressure reaches a certain value and holds constant, the corner radius will also be constant with a certain value, and the corner-filling process will stop. Only the work-hardening effect affects the corner-filling process at room temperature. However, it is very different at elevated temperatures because the work-hardening effect and strain rate sensitivity affect the corner-filling process at the same time. When the pressure reaches a certain value and holds constant, the corner radius gets smaller and smaller. From the analysis of tensile behaviour of Ti-3Al-2.5V alloy tubes above, the flow stress decreases as the strain rate decreases at 700 °C, the work-hardening exponent (n value) ranges from 0.05 to 0.16, and the strain rate sensitivity exponent (m value) is 0.13 under strain rates ranging from 10^{-1} s^{-1} to 10^{-3} s^{-1}, which is evidence for the inference above.

According to the pressure loading paths, the corner-filling curves were divided into two stages: the pressurization stage, which lasted 10 s, and the constant pressure stage, which lasted 290 s. Curve fitting was conducted during the two stages to understand the effect of different pressure loading paths on the corner-filling behaviour better. After many attempts, it was found that the pressurization stages all fit into linear curves very well, and the constant pressure stages all fit into exponential curves very well. The fitted curves are shown in Fig. 8. The linear curves can be expressed as Eq. 2.

$$r = A + B{\cdot}t \tag{2}$$

where r is the corner radius, t is the forming time and A and B are coefficients, which are listed in Table 2. The exponential curves can be expressed as Eq. 3.

$$r = C{\cdot}e^{D{\cdot}t} + E \tag{3}$$

where r is the corner radius, t is the forming time and C, D and E are coefficients, which are listed in Table 3. It can be seen that the corner radius got smaller and smaller at a constant filling rate during the pressurization stage and the filling rate was higher at higher pressurization rates. However, the filling rate decreased obviously as the corner radius got smaller

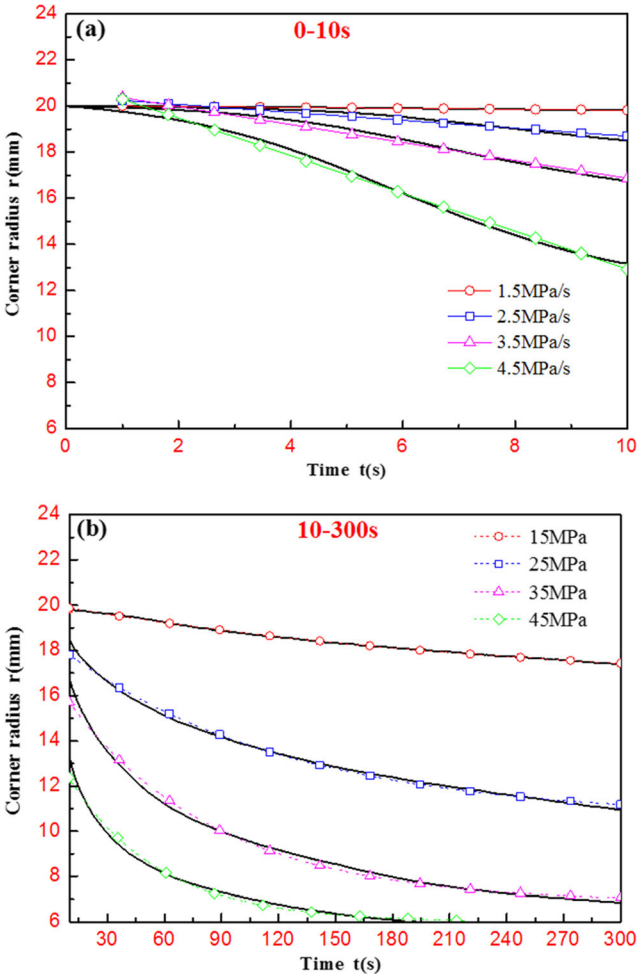

Fig. 8 Fitted corner-filling curves under various pressure loading paths and at 700 °C **a** pressurization stage and **b** constant pressure stage

during the constant pressure stage. As a corner radius gets smaller, it needs higher pressures to keep the filling rate stable. Even if the pressure holds constant, the strain rate will get lower to decrease the flow stress because of the strain rate sensitivity at elevated temperatures, and the corner will continue changing at a lower filling rate.

In order to investigate the effect of temperature on corner-filling behaviour further, the corner was formed, respectively, at temperatures of 650, 700, 750 and 800 °C, and the forming time was within 300 s. The same pressure loading path with the pressurization rate of 2.5 MPa s^{-1} was used at various temperatures. As shown in Fig. 9a, the repeatability of the same pressure loading path is satisfactory, and the pressure can be controlled within ±3 % of the target pressure.

Table 4 shows the corner radii of the tubular components formed at various temperatures, and Fig. 9b shows the corner-filling process. It can be seen that the filling rate is faster and the minimum corner radius is smaller at higher temperatures when using the same pressure loading path. Corner filling is easier because of decreased flow stress and weakened work-hardening effect at higher temperatures, which can be seen in

Table 2 The fitted results of pressurization stage at 700 °C

Pressurization rate (MPa s^{-1})	COF A	COF B	Fitting precision (%)
1.5	20.03	−0.02	98.57
2.5	20.42	−0.17	92.66
3.5	20.76	−0.39	97.51
4.5	21.12	−0.82	99.20

Figs. 4 and 6 above. It can also be seen that the corner-filling process does not stop at 650 °C when the pressure reaches 25 MPa and holds constant. This indicates that strain rate sensitivity starts to affect corner filling at 650 °C. The strain rate sensitivity exponent (*m* value) of 0.08, as shown in Fig. 6, is also evidence for this inference.

According to the pressure loading path, the corner-filling curves could also be divided into two stages: a pressurization stage of 10 s and a constant pressure stage of 290 s. In the same way, the two stages of the curves were fitted, respectively, to better understand the effect of temperature on corner-filling behaviour. It was also found that the pressurization stages all fit into linear curves very well, and the constant pressure stages all fit into exponential curves very well. The fitted curves are shown in Fig. 10. The linear curves can be expressed as Eq. 4.

$$r = A + B{\cdot}t \tag{4}$$

where r is corner radius, t is forming time and A and B are coefficients, which are listed in Table 5. The exponential curves can be expressed as Eq. 5.

$$r = C{\cdot}e^{D{\cdot}t} + E \tag{5}$$

where r is corner radius, t is forming time and C, D and E are coefficients, which are listed in Table 6. It can be seen that the corner radius got smaller and smaller at a constant filling rate during the pressurization stage and the filling rate was higher at a higher temperature.

During corner-filling process under various pressure loading paths and temperatures, the corner radius changed linearly over time during the pressurization stage (the pressurization rate was constant), but it changed exponentially over time during the constant pressure stage. The regularity of corner-filling behaviour in the HPPF process is obvious, but the filling behaviour itself is complicated because the work-hardening effect and strain rate sensitivity affect this behaviour at the same time during pneumatic forming at elevated temperatures. The high-pressure inflow process of gaseous medium also affects the behaviour because it can affect the temperature of the tube. This will be discussed further in section 3.3.

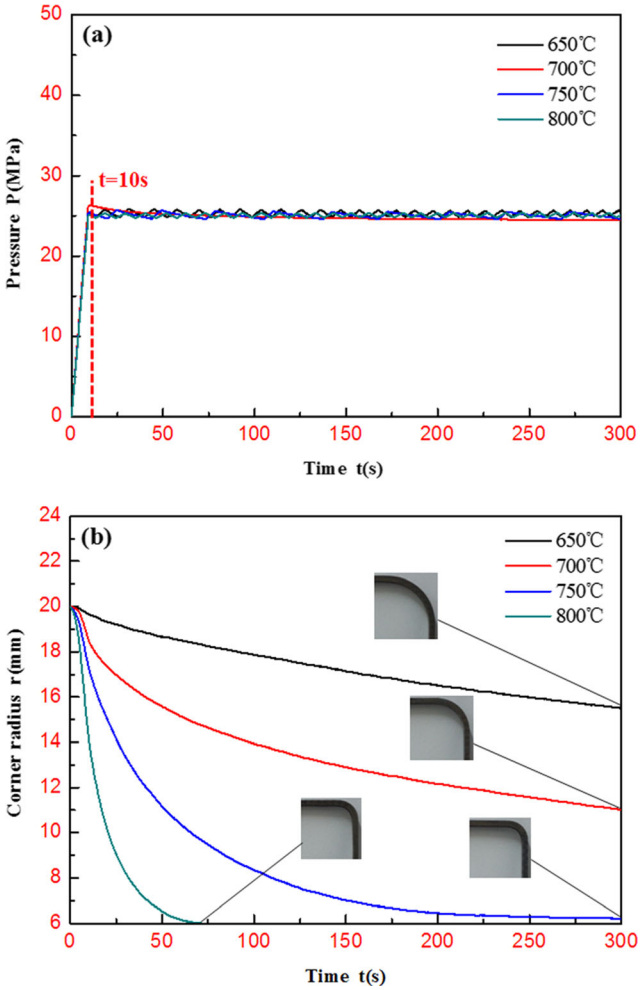

Fig. 9 **a** Pressure loading paths at various temperatures and with the same pressurization rate and **b** corner-filling curves at various temperatures

3.3 The influence of gaseous medium with high pressure on tube temperature

The high level of turbulence of inflowing gas causes the average heat transfer coefficient between the active medium and the work piece to be large enough. This should not be

Table 3 The fitted results of constant pressure stage at 700 °C

Constant pressure (MPa)	COF C	COF D	COF E	Fitting precision (%)
15	3.71	−0.004	16.32	99.89
25	7.87	−0.009	10.57	99.54
35	10.06	−0.013	6.83	99.31
45	7.86	−0.021	5.99	99.01

Table 4 Corner radii at various temperatures in 300 s

Temperature (°C)	Time (s)	Pressurization rate (MPa s^{-1})	Corner radius (mm)
650	300	2.5	15.5
700	300	2.5	11
750	300	2.5	6.2
800	300	2.5	6

Table 5 The fitted results of pressurization stage at various temperatures

Temperature (°C)	COF A	COF B	Fitting precision (%)
650	20.07	−0.04	97.06
700	20.42	−0.17	92.66
750	20.55	−0.31	97.03
800	21.26	−0.68	97.39

neglected during the HPPF process in spite of gas' low thermal conductivity [14]. In our previous work about the HPPF process of Ti-3Al-2.5V alloy parts with square cross-sections [15], there was a preforming process during the closing of the die because of the mere 10 % circumferential expansion ratio. After preforming, the tube significantly came into contact with the die cavity, and the cooling effect of the inflowing gas on the tube could be ignored because of the strong heat conduction between the tube and the isothermal die. In this study, however, the situation was very different. The circumferential expansion ratio increased to 20 %, and no preforming process would occur during the closing of the die. There was only line contact between the die cavity and tube, as shown in Fig. 1. Without the strong heat conduction at the beginning, the inflowing high-pressure gas would influence the tube temperature during the pneumatic forming process.

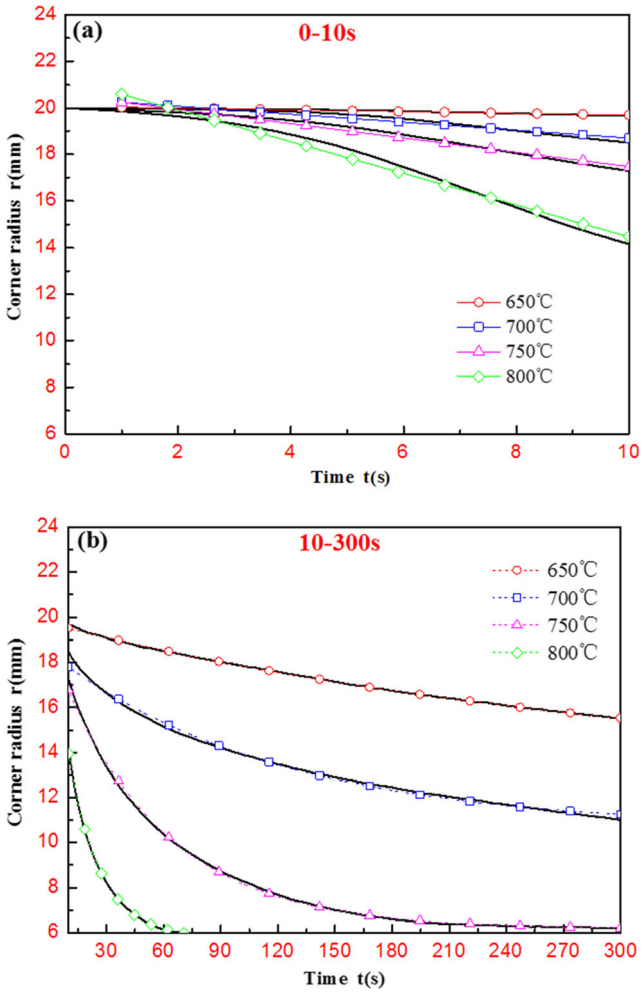

Fig. 10 Fitted corner-filling curves at various temperatures **a** pressurization stage and **b** constant pressure stage

During the gas bulge forming process, the tube came into contact with the straight wall area of die cavity first, and the tube temperature in this area became consistent with the die temperature immediately due to the strong and direct heat conduction between the tube and die. Therefore, the temperature at the straight wall area of the die cavity corresponded to the temperature at the straight wall area of tubular component. Actually, the temperatures of two typical points on the tubular component can be measured accurately based on the two thermocouples and the measuring method we adopted, viz the temperature at the centre of straight wall area and the temperature at the centre of corner area.

The results of the recorded temperature measurements and pressure loading paths are shown in Fig. 11, where T_s refers to the temperature at the centre of straight wall area and T_c refers to the temperature at the centre of the corner area. As shown in Fig. 11a, when the gas flowed into the tube at a pressurization rate of 0.194 MPa s^{-1} (with a 180 s pressure build-up time), T_c descended from 700 °C immediately, but T_s almost held constant. This is because the direct contact with the straight wall centre of the die cavity at the beginning and the strong heat conduction at this point counteracted the cooling effect of the inflowing gas. A temperature difference between the centre of the straight wall area and the corner area occurred, and the maximum value could reach 9 °C. With a very long pressure build-up time, the pressure presented a stair pattern of continuously rising, and 0.194 MPa s^{-1} was an average pressurization rate. At the same time, the isothermal die heated the tube

Table 6 The fitted results of constant pressure stage at various temperatures

Temperature (°C)	COF C	COF D	COF E	Fitting precision (%)
650	6.82	−0.003	12.91	99.95
700	7.87	−0.009	10.57	99.54
750	12.70	−0.018	6.16	99.89
800	14.97	−0.061	5.81	99.96

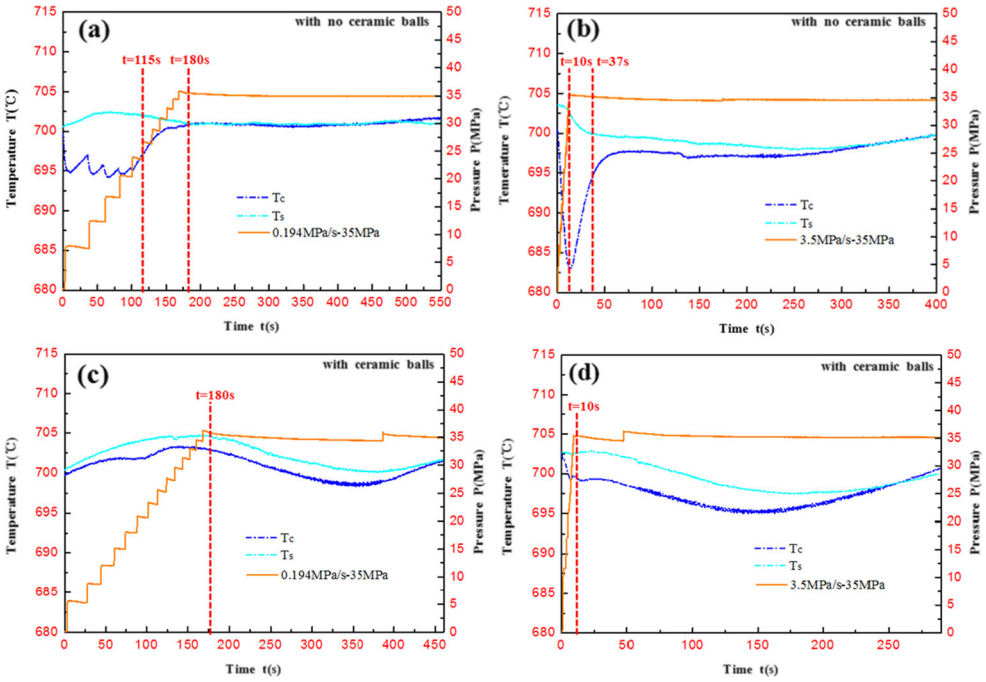

Fig. 11 Temperature curves of the centre of corner area and straight wall area of the tubular parts under four forming conditions **a** with no ceramic balls and 0.194 MPa s^{-1}–35 MPa, **b** with no ceramic balls and 3.5 MPa s^{-1}–35 MPa, **c** with ceramic balls and 0.194 MPa s^{-1}–35 MPa and **d** with ceramic balls and 3.5 MPa s^{-1}–35 MPa

continuously. Combined with the two effects, T_c undulated during the inflow process and reached agreement with T_s at the beginning of the constant pressure stage. However, when the gas flowed into the tube at a pressurization rate of 3.5 MPa s^{-1} (with a 10-s pressure build-up time), the cooling effect of the inflowing gas became much more obvious, and even T_s descended slightly. The maximum temperature difference between the centre of the straight wall area and the corner area could reach 19 °C. This is shown in Fig. 11b. At the end of pressurization stage, T_c descended to the minimum value, and it reached agreement with T_s during the constant pressure stage.

Inspired by the high-temperature air combustion technology, which adopted regenerative materials to preheat the air or gas fuel to a specific temperature previous to fuel combustion [18], the regenerative ceramic balls were filled into the tube to heat the inflowing gas. This method could also reduce the gas volume required to reach equal pressure. As expected, when the gas flowed into the tube at a pressurization rate of 0.194 MPa s^{-1} (with a 180-s pressure build-up time), the T_c and T_s of the tube filled with ceramic balls both held constant. This is shown in Fig. 11c. Even when the gas flowed into the tube at a pressurization rate of 3.5 MPa s^{-1} (with a 10-s pressure build-up time), the T_c of the tube filled with ceramic balls only descended a little, and the difference between T_c and T_s was within 3 °C, which could be ignored and considered to be isothermal. This is shown in Fig. 11d. When the die was heated up to 700 °C, the frequency of the induction heating unit had to be adjusted intermittently to keep the die temperature constant. The control accuracy was ±5 °C. Because of this, it was found that the temperature curves fluctuated slowly, except for the sharp fluctuation caused by inflowing gas, as shown in Fig. 11. Reaching the same constant pressure, the temperature difference is larger with a higher pressurization rate, and filling the tube with ceramic balls is an effective way to decrease or even eliminate the difference.

The corner-filling curves corresponding to the four forming conditions in Fig. 11 are shown in Fig. 12. The cross-section of the hollow part formed at a pressurization rate of 3.5 MPa s^{-1} with no ceramic balls is shown in Fig. 13. With no ceramic balls filled in the tube, the corner-filling process was faster with higher pressurization rates. It took 400 s to fully form the corner at 3.5 MPa s^{-1}, but it took 550 s at 0.194 MPa s^{-1}. The shapes of the corner-filling curves when the tubes were filled with ceramic balls were similar to the shapes of those formed with nothing in the tube, but the filling

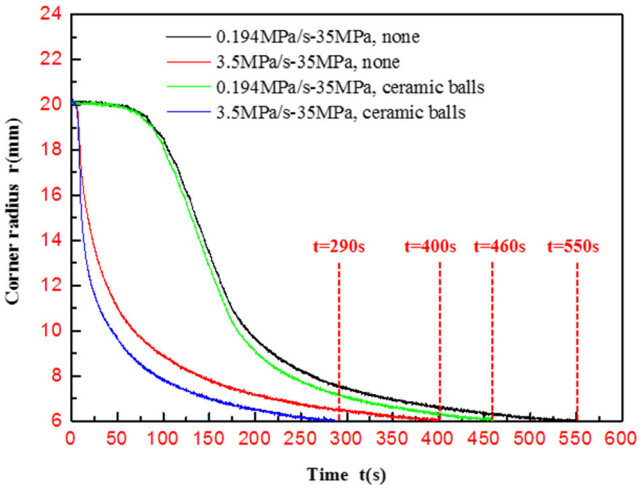

Fig. 12 Corner-filling curves under four forming conditions

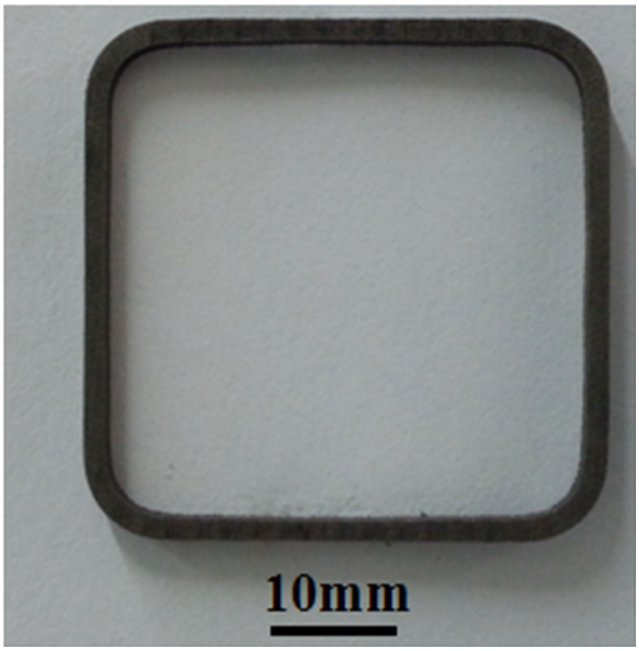

Fig. 13 The cross-section of the hollow part fully formed with the pressurization rate of 3.5 MPa s^{-1} and no ceramic balls

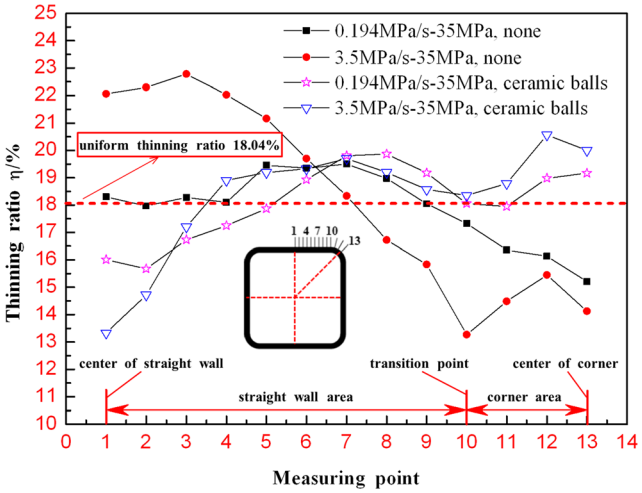

Fig. 14 Thickness profiles under four forming conditions

time was shorter. It took 290 s to fully form the corner at 3.5 MPa s^{-1} and 460 s at 0.194 MPa s^{-1}. In the gas forming process at elevated temperature, the strain rate is higher with higher pressure, so the forming time required is shorter. With higher pressurization rate, the pressure is higher at the same time, as shown in Fig. 11, so the strain rate is higher and the time required is shorter.

In Fig. 11a, it can be seen that the circular temperature difference between the centre of the straight wall area and the corner area came into being immediately as the gas flowed into the tube, and it lasted for 115 s. During this time period, the corner radius decreased from 20 to 16 mm, as shown in Fig. 12. Because of this, there was a non-isothermal stage (corner radius decreasing from 20 to 16 mm) during the whole corner-filling process. The same situation can be seen in Figs. 11b and 12, where the circular temperature difference lasted for 37 s and the corner radius decreased from 20 to 12 mm. With no ceramic balls filled in the tube, the cooling effect of the inflowing gas is obvious, even with a very slow pressurization rate. However, with ceramic balls filled in the tube, the cooling effect of the inflowing gas could be eliminated in this study, and the whole corner-filling process was isothermal. With the same pressurization profile, the flow stress is larger and strain rate is lower at lower temperatures. This is why the isothermal corner-filling process is faster than the non-isothermal corner-filling process.

The thickness profiles of the tubular components corresponding to the four forming conditions in Fig. 11 were also analysed, as shown in Fig. 14. Considering the symmetry of the die cavity with a square cross-section, an eighth of the component was analysed. With no ceramic balls filled in the tube, deformation at the straight wall area was found to be larger than that at the corner area. This was caused by temperature difference between the centre of the straight wall area and the corner area during the HPPF process. At 3.5 MPa s^{-1}, the maximum thinning ratio was 22.8 %, and it occurred close to the centre of straight wall area. The minimum thinning ratio was 13.3 % and it occurred close to the centre of corner area. At 0.194 MPa s^{-1}, however, the thickness uniformity was improved to a certain degree. The maximum and minimum thinning ratios were 19.5 and 15.2 %, respectively. Furthermore, the position where the maximum thinning ratio occurred shifted to the transition point between the centre of the straight wall area and the corner area to a certain degree. This is very different from hydroforming at room temperature, in which the maximum thinning ratio usually occurs close to the transition point between the centre of the straight wall area and the corner area [19]. The non-isothermal stage resulted in this case. During this stage, the straight wall area deformed more easily because of the higher temperature. Lower strain rates, smaller friction forces and smaller temperature differences at lower pressurization rates could provide more uniform thickness profiles.

With ceramic balls filled in the tube, the whole process was isothermal, and the thickness profile was similar to that of hydroforming at room temperature. At 3.5 MPa s^{-1}, the maximum thinning ratio was 20.6 %, and it occurred close to the transition point; the minimum thinning ratio was 13.3 %, and it occurred close to the centre of straight wall area. At 0.194 MPa s^{-1}, the thickness uniformity was improved slightly. The maximum and minimum thinning ratios were 19.9 and 15.7 %, respectively. This case was caused by lower strain rates and smaller friction forces at lower pressurization rates [15, 20]. With the same pressure loading path to eliminate the influence of friction force, it was also found that temperature difference affects the thickness profile significantly, which can

be seen by comparing the thickness profiles of tubes formed in isothermal and non-isothermal conditions. Adopting a lower pressurization rate is effective for improving thickness uniformity, especially in the pneumatic forming process with no regenerative materials in the tube. Filling regenerative materials into the tube was found to be an effective way of decreasing or eliminating temperature differences.

4 Conclusions

The HPPF system was further developed based on previous work. The results of HPPF experiments indicate that this system can provide accurate pressure control within ±3 % of the target pressure.

The flow stress of Ti-3Al-2.5V tubes decreases with the decrease of strain rate and the increase of deformation temperature at elevated temperature. The fracture elongation is above 70 % even at strain rates of up to 10^{-1} s^{-1} at 700 °C, which indicates that it is suitable for the HPPF process of Ti-3Al-2.5V alloy tubes at temperatures below 800 °C.

Based on the accurate pressure control, the corner-filling process can be divided into pressurization stage and constant pressure stage. Under various pressure loading paths and temperatures, the corner radii all change linearly over time during the pressurization stage, but they change exponentially over time during the constant pressure stage.

During the HPPF process, the cooling effect of inflow gas on the tube is obvious. Because the straight wall area of the part comes into contact with the die first, there is temperature difference between the centre of the straight wall area and the corner area during the inflow process. Because of this, deformation at the straight wall area is greater than that at the corner area. Adopting the lower pressurization rate and filling regenerative materials into the tube are effective for decreasing or eliminating the temperature difference.

Acknowledgments The authors would like to thank for the supports from the Innovative Research Team in University (No. IRT1229) and Program for Changjiang Scholars.

References

1. Leyens C, Peters M (2003) Titanium and titanium alloys. Wiley-VCH, Weinheim
2. Yang H, Fan XG, Sun ZC, Guo LG, Zhan M (2011) Recent developments in plastic forming technology of titanium alloys. Sci China Technol Sci 54:490–501
3. Odenberger EL, Pederson R, Oldenburg M (2008) Thermomechanical material response and hot sheet metal forming of Ti-6242. Mater Sci Eng A 489:158–168
4. Huang W, Zan X, Nie X, Gong M, Wang Y, Xia YM (2007) Experimental study on the dynamic tensile behavior of a polycrystal pure titanium at elevated temperatures. Mater Sci Eng A 443:33–41
5. Tsao LC, Wu HY, Leong JC, Fang CJ (2012) Flow stress behavior of commercial pure titanium sheet during warm tensile deformation. Mater Des 34:179–184
6. Zhang ZY, Yang H, Li H, Ren N, Wang D (2013) Quasi-static tensile behavior and constitutive modeling of large diameter thin-walled commercial pure titanium tube. Mater Sci Eng A 569:96–105
7. Luo Y, Luckey SG, Friedman PA, Peng Y (2008) Development of an advanced superplastic forming process utilizing a mechanical pre-forming operation. Int J Mach Tools Manuf 48:1509–1518
8. Luckey G Jr, Friedman P, Weinmann K (2009) Design and experimental validation of a two-stage superplastic forming die. J Mater Process Technol 209:2152–2160
9. Luo Y, Luckey SG, Copple WB, Friedman PA (2008) Comparison of advanced SPF die technologies in the forming of a production panel. J Mater Eng Perform 17:142–152
10. Liu J, Tan MJ, Aue-u-lan Y, Guo ML, Castagne S, Chua BW (2013) Superplastic-like forming of Ti-6Al-4V alloy. Int J Adv Manuf Technol 69:1097–1104
11. Tang JS, Fuh YK, Lee S (2015) Superplastic forming process applied to aero-industrial strakelet: wrinkling, thickness, and microstructure analysis. Int J Adv Manuf Technol 77:1513–1523
12. Neugebauer R, Schieck F (2010) Active media-based form hardening of tubes and profiles. Prod Eng Res Devel 4:385–390
13. Elsenheimer D, Groche P (2009) Determination of material properties for hot hydroforming. Prod Eng Res Devel 3:165–174
14. Drossel WG, Pierschel N, Paul A, Katzfuß K, Demuth R (2014) Determination of the active medium temperature in media based press hardening processes. J Manuf Sci Eng 136:1–8
15. Liu G, Wang JL, Dang KX, Tang ZJ (2014) High pressure pneumatic forming of Ti-3Al-2.5V titanium tubes in a square cross-sectional die. Materials 7:5992–6009
16. Liu G, Wang KH, Xu Y, Wang B, Yuan SJ (2013) An approach to improve thickness uniformity of TA15 tubular part formed by gas bulging process. Adv Mater Res 712:651–657
17. Wu HY, Hsu WC (2010) Tensile flow behavior of fine-grained AZ31B magnesium alloy thin sheet at elevated temperatures. J Alloys Compd 493:590–594
18. Pan LM, Ji HC, Cheng SM, Wu CB, Yong HQ (2009) An experimental investigation for cold-state flow field of regenerative heating annular furnace. Appl Therm Eng 29:3426–3430
19. Hwang YM, Chen WC (2005) Analysis of tube hydroforming in a square cross-sectional die. Int J Plast 21:815–1833
20. Wu HY, Tzou MD, Huang CC, Tsai HH (2015) Modified male die rapid gas blow forming of fine-grained Mg alloy AZ31B thin sheet. Int J Adv Manuf Technol 80:1241–1252